Forming the Phosphate Layer in Reconstituted Horse Spleen Ferritin and the Role of Phosphate in Promoting Core Surface Redox Reactions[†]

Joseph L. Johnson,[‡] Michelle Cannon,[§] Richard K. Watt,[§] Richard B. Frankel,[||] and Gerald D. Watt*,[‡]

Department of Chemistry and Biochemistry and Undergraduate Research Program, Brigham Young University, Provo, Utah 84602, and Department of Physics, California State Polytechnic University, San Luis Obispo, California 93407

ABSTRACT: Apo horse spleen ferritin (apo HoSF) was reconstituted to various core sizes (100–3500 Fe^{3+}/ HoSF) by depositing $Fe(OH)_3$ within the hollow HoSF interior by air oxidation of Fe^{2+}. Fe^{2+} and phosphate (P_i) were then added anaerobically at a 1:4 ratio, and both Fe^{2+} and P_i were incorporated into the HoSF cores. The resulting P_i layer consisted of Fe^{2+} and P_i at about a 1:3 ratio which is strongly attached to the reconstituted ferritin mineral core surface and is stable even after air oxidation of the bound Fe^{2+}. The total amount of Fe^{2+} and P_i bound to the iron core surface increases as the core volume increases up to a maximum near 2500 iron atoms, above which the size of the P_i layer decreases with increasing core size. Mössbauer spectroscopic measurements of the P_i-reconstituted HoSF cores using $^{57}Fe^{2+}$ show that $^{57}Fe^{3+}$ is the major species present under anaerobic conditions. This result suggests that the incoming $^{57}Fe^{2+}$ undergoes an internal redox reaction to form $^{57}Fe^{3+}$ during the formation of the P_i layer. Addition of bipyridine removes the $^{57}Fe^{3+}$ bound in the P_i layer as $[^{57}Fe(bipy)_3]^{2+}$, showing that the bound $^{57}Fe^{2+}$ has not undergone irreversible oxidation. This result is related to previous studies showing that $^{57}Fe^{2+}$ bound to native core is reversibly oxidized under anaerobic conditions in native holo bacterial and HoSF ferritins. Attempts to bury the P_i layer of native or reconstituted HoSF by adding 1000 additional iron atoms were not successful, suggesting that after its formation, the P_i layer "floats" on the developing iron mineral core.

Native ferritins isolated from plant, animal, and bacterial sources are all composed of 24 subunits and contain large amounts of iron in the form of an iron oxy–hydroxy mineral core sequestered within the hollow protein interiors (*1–3*). Phosphate is also associated with native mineral cores, but the amount present is dependent upon the biological source of the ferritins (*4–6*). Horse spleen ferritin (HoSF)[1] contains on average about one phosphate per 10 iron atoms (*7*), and the phosphate appears to be surface-bound; on the other hand, bacterial ferritin cores contain phosphate-to-iron ratios of ∼1 (*6*) with the phosphate uniformly distributed (*8*) throughout the mineral core. The role of phosphate in ferritin mineral cores is not known, nor is the physiological process by which phosphate is incorporated. Although both animal and bacterial ferritins can be reconstituted in vitro in the absence of

phosphate (*4*), the presence of naturally occurring phosphate has a pronounced effect (*2*, *3*) on the crystallinity, chemical reactivity, and spectroscopic properties of the mineral cores. These observations demonstrate that although phosphate is not essential for core formation, its presence influences mineral core properties and likely has a physiological role in ferritin function.

Initial investigations of the physiological role of phosphate in ferritin function suggested that phosphate is involved in facilitating ferritin core formation and assisting in redox reactions. Cheng and Chasteen (*9*) reported that phosphate accelerated both the rate of oxidation of Fe^{2+} to form individual Fe^{3+} ions and also directed the transfer of this mononuclear Fe^{3+} to form oligomeric aggregates. Jacobs et al. (*10*) showed that the anaerobic addition of $^{57}Fe^{2+}$ to native, holo HoSF resulted in a reversible internal oxidation of added $^{57}Fe^{2+}$ to $^{57}Fe^{3+}$, suggesting that phosphate promotes redox reactions in native holo ferritin. Watt et al. (*11*) confirmed the phosphate-assisted redox reactivity in bacterial ferritin containing higher levels of phosphate in the ferritin cores. Huang et al. (*12*) reported that phosphate was not only responsible for Fe^{2+} binding to native HoSF cores but also that phosphate was readily released upon reduction of the core. These observations regarding phosphate-promoted iron core redox reactivity suggest that a redox surface is formed on the ferritin core involving both phosphate and surface-bound iron atoms. Such a redox active surface containing phosphate may be functional in catalyzing iron redox reactions associated with iron deposition and iron release

1 Abbreviations: HoSF, horse spleen ferritin; rHuHF, recombinant heavy human liver ferritin; DT, sodium dithionite; bipy, α,α-bipyridine; TES, *N*-tris(hydroxymethyl)methyl-2-aminoethanesulfonic acid; MOPS, 3-(*N*-morpholino)propanesulfonic acid; ICP, inductively coupled plasma; DES, deferoxamine mesylate or Desferal; P_i, phosphate group; FAB, fast atom bombardment; IR, infrared spectroscopy.

conducted by ferritins. A similar proposal has been made for P_i-free cores, and recent results have been interpreted to suggest that oxidation at high Fe^{2+} flux occurs on the mineral core surface and makes an important contribution to the overall catalytic iron deposition process in rHuHF and HoSF (*13*).

The reactions involving the redox active P_i surface discussed above were all conducted with ferritins containing native phosphate in their cores. Formation of a native P_i layer on reconstituted ferritin cores has not been reported, and the in vivo process for forming such a native P_i surface remains unknown. Here, we describe a method for forming a redox active, P_i surface on reconstituted HoSF cores and show that this reconstituted surface behaves in a manner similar to that found in native HoSF cores. In addition, the reactivity of the P_i mineral surface is examined and the relationship of the core size to the amount of reconstituted phosphate is evaluated. The properties of how this P_i surface behaves during iron deposition and release are also discussed.

MATERIALS AND METHODS

Horse Spleen Ferritins. Apo HoSF was either purchased directly from Sigma or made from holo HoSF by the thioglycollic acid method (*14*). Final removal of core iron from either apo HoSF source was carried out by reduction with DT in the presence of bipy followed by removal of $[Fe(bipy)_3]^{2+}$ either by Sephadex G-25 chromatography or by several concentration−dilution cycles with 0.025 M TES (pH 7.5) using an Amicon concentrator.

Reconstituted holo HoSF with core sizes ranging from 100 to 3500 Fe atoms/ferritin was prepared by stirring 5 mL portions of 5−10 mg/mL apo HoSF in 0.1 M TES or HEPES (pH 6.5−7.0) containing 0.1 M NaCl in air and adding 50 μL portions of 0.05 M Fe^{2+} every 5−10 min until the desired core size was attained. During core reconstitution, the pH was kept constant using 0.05 M NaOH. After core formation, reconstituted HoSF was stored for several hours or overnight at 4 °C, centrifuged to remove a faint cloudiness, and then passed through a 1.0 cm × 15 cm Sephadex G-25 column equilibrated with 0.025 M TES (pH 7.4) containing 0.1 M NaCl to remove any low-molecular mass Fe complexes. The protein concentration was measured by the Lowry method, and the iron content was determined after DT reduction from the absorbance of $[Fe(bipy)_3]^{2+}$ ($\epsilon_{520} = 8400$ cm^{-1} M^{-1}). During formation of holo HoSF with >2500 Fe atoms/HoSF, the rate of iron deposition in the core was much slower, causing the amount of non-ferritin-bound iron to become more significant as the core size increased. The particulate iron was removed as $Fe(OH)_3$ by centrifugation, and non-ferritin-bound iron remaining in solution was removed by repeated centrifugation through Centricon 300 filters (Amicon) with nominal cutoff values of 300 000 Da which retained reconstituted HoSF but removed soluble but non-specifically formed iron aggregates in the effluent. These iron-reconstituted HoSF samples were then characterized by Lowry and iron analysis.

Reconstitution of the Phosphate Layer. To 0.2−0.5 mL of anaerobic, iron-reconstituted HoSF (10 mg/mL) in 0.025 M TES (pH 7.5) was first added 0.01 M Fe^{2+} to make a 50−300-fold excess of Fe^{2+} over HoSF, followed by addition of a 0.01 M phosphate solution at pH 7.5 to give a P_i:Fe^{2+}

ratio of about 4:1. When the phosphate was added prior to the iron, a precipitate formed [presumably $FePO_4$ and/or $Fe_3(PO_4)_2$ which are both insoluble under these conditions] and the P_i layer was not formed. The mixture was incubated anaerobically in a Vacuum Atmospheres glovebox (O_2 level of <1.0 ppm) for 20−30 min and then eluted from an anaerobic Sephadex G-25 column (1.0 cm × 15 cm) equilibrated in 0.025 M TES (pH 7.5) to remove the excess Fe^{2+} and P_i. The amount of Fe^{2+} in HoSF was determined by the bipy method and phosphate using a Perkin-Elmer ICP emission spectrophotometer with appropriate phosphate standards. From these measurements, the P_i:Fe^{2+} ratio in the bound P_i layer was determined. P_i:Fe^{2+} ratios other than 4:1 were tried during the reconstitution procedure, but this ratio was most effective in reconstituting the P_i layer. This procedure was repeated for each iron-reconstituted HoSF sample, which spanned the range from 100 to 3500 iron atoms/HoSF. The anaerobic samples containing the reconstituted Fe^{2+}−P_i layer were then exposed to air to oxidize the bound Fe^{2+}, passed through another Sephadex G-25 column equilibrated in 0.025 M TES (pH 7.5), and reanalyzed for phosphate and total iron.

Location and Reactivity of the Reconstituted Phosphate Layer. To assess the Fe^{2+} binding ability of HoSF after reconstitution with phosphate and air oxidation, 1.0 mL of P_i-reconstituted HoSF was made anaerobic, excess Fe^{2+} (no phosphate) was added, and the mixture was incubated anaerobically for 20 min and then separated by Sephadex G-25 chromatography (*11*, *12*, *15*). The amount of Fe^{2+} that bound to the reconstituted P_i layer present in P_i-reconstituted HoSF was then determined by the bipy method. Parallel experiments with native HoSF were conducted to compare the Fe^{2+} binding ability of the P_i layers in native and P_i-reconstituted HoSF, each with similar sized cores and phosphate levels. A control reaction was carried out to determine if Fe^{2+} binds to P_i-free iron-reconstituted cores by adding excess Fe^{2+} and following the above separation procedures.

To determine if the native and reconstituted P_i layer in HoSF can be buried by incoming core iron atoms resulting from Fe^{2+} oxidation, 1.0 mL portions of each were stirred in air and 1000 additional iron atoms were deposited into the ferritin core by air oxidation of aliquots of added 0.1 M Fe^{2+}. These samples were made anaerobic, reacted with Fe^{2+}, and separated by anaerobic Sephadex G-25 chromatography, and the Fe^{2+} content was measured.

Non-Redox Iron Removal from HoSF by Desferal. The chelation of Fe^{3+} by DES from native HoSF containing 1600−2250 iron atoms and 250−300 phosphate ions per mineral core was conducted by reacting 0.25 mL of native HoSF in 0.1 M TES or MOPS (pH 7.5) with a 1−5-fold excess of DES over Fe in HoSF, allowing the reaction to occur for 2−24 h, and then isolating the resulting HoSF by Sephadex G-25 chromatography. The iron and phosphate content of this series of altered HoSF samples were then determined to evaluate how phosphate loss correlated with iron loss by nonreductive iron chelation. Fe^{2+} binding under anaerobic conditions was then carried out as described above to assess the presence and reactivity of the surface P_i layer.

Mössbauer Spectroscopy. Reconstituted HoSF with 1100 iron atoms present in the core was reacted with excess P_i and $^{57}Fe^{2+}$ at a 4:1 ratio. After reaction, the mixture was

Table 1: P_i and Fe^{2+} Binding during P_i Reconstitution of Iron-Reconstituted HoSF

HoSF core size[a] (no. of iron atoms/HoSF)	no. of P_i atoms bound	no. of Fe^{2+} atoms bound	$P_i:Fe^{2+}$
100	35	9	3.9
500	178	51	3.5
850	280	72	3.9
1059	361	81	4.5
1600	385	105	3.7
2100	612	140	4.4
2500	585	85	4.9
3013	350	55	6.0
3400	330	42	7.8

[a] The results in this table are taken from Figure 1.

separated as described above, concentrated to 35 mg/mL, transferred to a 1.0 cm Mössbauer cell, and frozen in liquid nitrogen. As a control reaction, an identical sample of P_i-free reconstituted HoSF was reacted as above with excess $^{57}Fe^{2+}$ and loaded into another Mössbauer cell and frozen for analysis. Mössbauer spectra were recorded as previously described (*15*).

Mass Spectrometry. Mass spectrometric measurements were performed on a JEOL SX102A double-sector mass spectrometer using FAB. A small portion of the Mössbauer sample was retained and reacted with bipy to quantify the relative amount of added $^{57}Fe^{2+}$ recovered as $[^{57}Fe(bipy)_3]^{2+}$ and to account for any $^{57}Fe^{2+}$ that was inadvertently oxidized during sample preparation.

RESULTS

Phosphate Layer Reconstitution. The anaerobic addition of excess Fe^{2+} followed by phosphate at a 1:4 ratio to iron-reconstituted HoSF causes both Fe^{2+} and P_i to enter the ferritin interior and to apparently deposit on the iron mineral core surface, forming a P_i layer with a stoichiometry of about 3−5 phosphates per added Fe^{2+} (Table 1). If a $P_i:Fe^{2+}$ ratio of less than 4:1 is used, all the phosphate is incorporated while the excess Fe^{2+} remains free and is easily separated from P_i-reconstituted HoSF. If a ratio of more than 4:1 is used, the $Fe^{2+}-P_i$ layer forms with the same 3−5 P_i per Fe^{2+} stoichiometry while the excess phosphate is removed during the Sephadex G-25 chromatography step. These experiments clearly indicate that both P_i and Fe^{2+} are simultaneously required (at an ~4:1 ratio) under anaerobic conditions for proper reconstitution of the P_i-Fe layer. Exposure of anaerobic reconstituted HoSF containing the bound Fe^{2+} and P_i layer to air results in oxidation to Fe^{3+} with retention of the phosphate. When reconstituted anaerobically, the bound Fe^{2+} in the P_i layer is stable but is readily removed upon addition of excess bipy as the $[Fe(bipy)_3]^{2+}$ complex, with concomitant release of the bound phosphate.

P_i and Fe^{2+} Binding as a Function of Core Size. The relationship between the amount of P_i and Fe^{2+} bound as a function of ferritin core size was next investigated. Figure 1 shows that for core sizes ranging from 100 to 2300−2700 atoms, the amounts of bound P_i and Fe^{2+} exhibit the same general trend as a function of core size. At about 2300−2700 iron atoms per ferritin core, maximum binding of both P_i and Fe^{2+} is observed, followed by a decline for both. Table 1 summarizes the $P_i:Fe^{2+}$ stoichiometry of the reconstituted P_i layer shown in Figure 1 as a function of core size. The
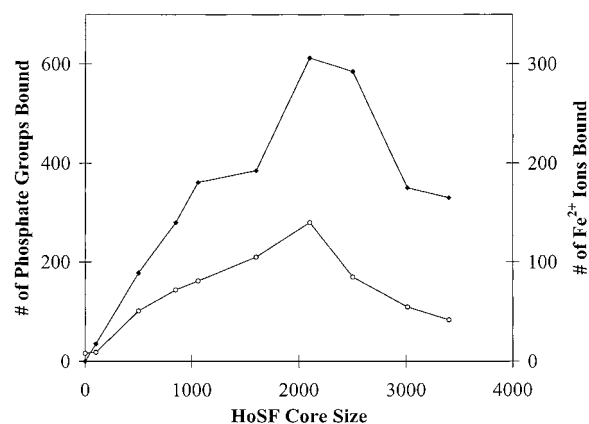

FIGURE 1: Reconstitution of the P_i layer in iron-reconstituted HoSF. The number of phosphate groups bound, after the anaerobic addition of Fe^{2+} and P_i to iron-reconstituted HoSF as described in the text, is plotted as a function of HoSF core size (left y-axis, ◆). The amount of Fe^{2+} ions bound to the P_i layer after reconstitution is also plotted as a function of HoSF core size (right y-axis, ○). The solid lines simply connect the data points and have no theoretical significance.

Table 2: Fe^{2+} Binding to Fe-Reconstituted (No P_i) and P_i-Reconstituted (with P_i) HoSF

HoSF core size[a] (no. of iron atoms/HoSF)	no. of Fe^{2+} atoms/HoSF[b] (no P_i)	no. of Fe^{2+} atoms/HoSF[c] (with P_i)	no. of P_i atoms/ HoSF[d]	$P_i:Fe^{2+}$[e]
0 (apo)	8.1	8.0	<1.0	≈0
500	5.6	14.1	42.2	3.3
620	7.2	15.4	41.1	4.2
1000	7.9	20.2	78.2	3.9
1500	6.2	38.3 (35)	110	2.9
2160	7.2	31.0 (41)	129	2.8
2500	−	45.0 (50)	160	3.6
3010	8.4	49.1	176	3.6
3626	−	37	96	2.6

[a] The number of iron atoms in the core of iron-reconstituted HoSF. [b] Number of Fe^{2+} ions bound to iron-reconstituted HoSF in the absence of phosphate. [c] Number of Fe^{2+} ions bound to P_i-reconstituted HoSF as outlined above. After reconstitution, the HoSF was oxidized in air and made anaerobic, and then the extent of Fe^{2+} binding shown in this column was determined. Values in parentheses are from duplicate experiments. [d] Number of phosphate groups present after P_i reconstitution. [e] The amount of phosphate groups bound per bound Fe^{2+}.

$P_i:Fe^{2+}$ stoichiometry is nearly constant at 4.0 for core sizes up to 2500 iron atoms, after which the amount of P_i bound per Fe^{2+} appears to increase. This apparent increase in the $P_i:Fe^{2+}$ stoichiometry may not be significant because in other experiments (see Table 2), the $P_i:Fe^{2+}$ stoichiometry remained constant near 4.0 throughout the range of core sizes that were examined. This uncertainty may arise because HoSF containing more than 2500 iron atoms per core is more difficult to prepare than that containing smaller cores. In addition, the decrease in the amount of bound Fe^{2+} with increasing core size above 2500 atoms makes colorimetric quantification of Fe^{2+} in the presence of large cores more difficult due to larger blank corrections from core iron absorption.

To assess the repeatability of the results depicted in Figure 1, a total of four separate experiments were conducted with independently reconstituted HoSF samples spanning the same range of core sizes. In each of these four separate experiments, the same overall behavior as reported in Figure 1 was observed with the extent of both P_i and Fe^{2+} binding

increasing up to core sizes of near 2500 Fe atoms/HoSF, after which both decrease with increasing core size. However, the amount of phosphate bound in these independent experiments differed from that shown in Figure 1 and Table 1. Of the four phosphate reconstitution experiments conducted, the results in Figure 1 and Table 1 represent the highest phosphate binding levels observed with phosphate levels comparable to or higher than phosphate levels in native HoSF.

The results in Table 2 represent the lowest phosphate levels observed in P_i-reconstituted HoSF samples and are about one-fourth of the phosphate values reported in Figure 1 (compare column 2 of Table 1 with column 4 of Table 2). The other two experiments (not shown) gave intermediate levels of phosphate binding to iron-reconstituted HoSF. Within each of the four HoSF reconstitution experiments, the P_i:Fe^{2+} stoichiometry was constant but varied from that reported in Table 1, ranging typically from as low as 2.0 to more than 4.5 as seen in Table 1. Thus, while similar results from a given set of reconstituted HoSF samples were overall consistent with the results shown in Figure 1, the amount of reconstituted phosphate that was present differed depending on the reconstituted HoSF samples that were used. The cause of this variable behavior is not readily discerned from the experiments described here but is likely due to the differing core properties resulting from different conditions occurring during reconstitution. Although attempts were made to standardize and control reconstitution conditions during core formation, variables such as O_2 concentration, local pH changes, rates of Fe^{2+} oxidation, and subsequent $Fe(OH)_3$ formation and deposition are difficult to control and likely lead to variable core properties. Variation in core properties such as particle sizes, the number of nucleation sites, the mineral density, and the degree of crystallinity will likely influence the surface area of the mineral core onto which the P_i layer is deposited, resulting in the observed variation.

The anaerobic addition of excess phosphate alone to reconstituted HoSF, followed by anaerobic Sephadex G-25 chromatography, produces HoSF containing no appreciable phosphate associated with the reconstituted iron core. However, anaerobic Fe^{2+} addition to apo or iron-reconstituted HoSF indicates that about 8.0 Fe^{2+} atoms bind independent of the presence or absence of the iron-reconstituted core (see Table 2), suggesting that 8.0 Fe^{2+} atoms strongly bind at protein and not core surface sites. However, this result does not preclude the possibility of weak Fe^{2+} binding to the core, and evidence presented below indicates that weak binding of Fe^{2+} to the P_i-free mineral core may occur.

Phosphate Layer Reactivity. Having prepared P_i-reconstituted HoSF with cores closely resembling native cores and demonstrating that the cores are functional in binding added Fe^{2+} under anaerobic conditions, we attempted to further characterize the reactivity of the P_i layer. The P_i layer in both native and reconstituted HoSF is assumed to be the site where Fe^{2+} binding occurs (*12*), and it is further assumed that the P_i layer resides on the mineral core surface. If 1000 additional iron atoms are added to either native or P_i-reconstituted HoSF containing the surface-bound P_i layer, such an extensive iron deposition could bury the P_i layer, rendering it incapable of binding incoming Fe^{2+}. However, if the P_i layer remains surface-bound by catalytically transferring the incoming iron to the iron core surface below

Table 3: Two Independent Experiments of Fe^{2+} Binding to Native Holo and Native Holo Containing 1000 Additional Fe Atoms

HoSF sample	no. of Fe^{2+} atoms/HoSF[d]	no. of P_i atoms/HoSF	P_i:Fe^{2+}
native 1[a]	137 ± 23	545 ± 50	4.0
native 1 and P_i[b]	173 ± 15	474 ± 25	2.7
native 1 and 1000 Fe[c]	218 ± 40	451 ± 30	2.1
native 2[a]	126 ± 25	392 ± 15	3.3
native 2 and P_i[b]	198 ± 16	376 ± 15	1.9
native 2 and 1000 Fe[c]	136 ± 8	395 ± 15	2.9

[a] Two independent holo HoSF samples were used. [b] Each HoSF sample was treated with Fe^{2+} and P_i as outlined in the text to maximally reconstitute the P_i layer in native HoSF. [c] An additional 1000 iron atoms were deposited in each native HoSF sample by air oxidation of Fe^{2+} at pH 7.4 in 0.10 M TES. [d] The amount of Fe^{2+} that bound to the indicated HoSF species. The values are the average of triplicate measurements.

it, then an undiminished level of Fe^{2+} binding would be expected. If partial burial of the P_i layer occurs, intermediate levels of Fe^{2+} binding between these two extremes would be expected.

Table 3 shows results of two separate experiments (native 1 and native 2) in which we compare the Fe^{2+} binding ability of (a) native HoSF, (b) native HoSF reconstituted by adding additional phosphate by the $Fe^{2+}-P_i$ method described above, and (c) native HoSF to which an additional 1000 iron atoms have been added aerobically. The results in the first column clearly show that Fe^{2+} binding to native HoSF is extensive and nearly identical with previous results for native HoSF (*10*). The second and fifth rows in the first column show that the level of Fe^{2+} binding increases when additional phosphate is added. When an additional 1000 iron atoms are added to native HoSF, the Fe^{2+} binding capacity remains essentially unchanged, as is seen by comparing rows 3 and 6 of column 1, suggesting that the phosphate is still exposed and able to bind Fe^{2+}. The apparent increase in the level of Fe^{2+} binding over the native level in the first experiment is nearly within the error overlap, and we do not consider it significant. The second column shows that the amount of phosphate initially present remains associated with HoSF after 1000 additional iron atoms are added. The third column shows that 2.0−3.0 phosphates bind per incoming Fe^{2+}, in agreement with earlier results (*10*) and with the results listed in Tables 1 and 2. When native HoSF containing its naturally occurring P_i layer is treated using the above reconstitution conditions, up to 20% more phosphate can be added (depending on the native HoSF sample), indicating that not all of the iron core surface in native HoSF was initially covered.

Fe^{3+} Removal with Desferal. The reaction of DES with oxidized native HoSF slowly removes Fe^{3+} from the mineral core at pH 7.5 via the nonredox reaction shown in eq 1.

$$Fe(OH)_3 \text{ (core)} + H_4DES^+ = FeHDES^+ + 3H_2O \quad (1)$$
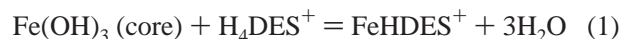
It is interesting to compare the role of phosphate in this nonredox iron removal reaction with the presumed physiologically relevant redox-assisted iron removal reaction. In the latter case, 60% of the phosphate is removed when 10% of the native ferritin core is reduced (*12*). An important question regarding iron removal from the HoSF core by nonreductive chelation focuses on whether the P_i layer remains in place and possibly assists in iron removal or whether it is removed
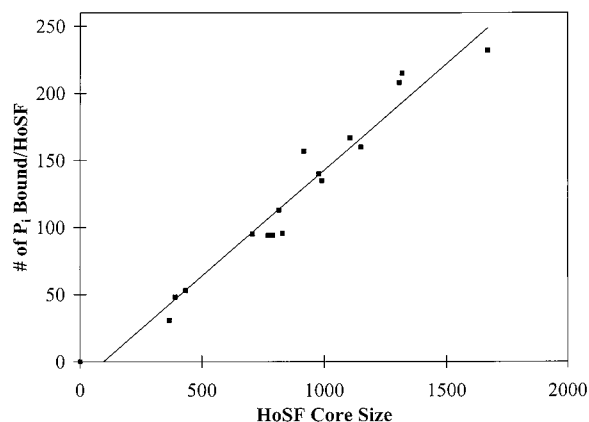
FIGURE 2: Removal of iron and phosphate from native HoSF by Desferal (DES) chelation. The number of phosphate groups that remained bound to HoSF is plotted as a function of HoSF core size. Native HoSF ferritin containing 1675 iron atoms and 230 phosphate groups was reacted with excess DES for various amounts of time and separated by Sephadex G-25 chromatography, and the amounts of bound Fe^{2+} and P_i were determined. The solid line is a least-squares fit giving a slope of 0.16 ± 0.01 P_i:Fe.
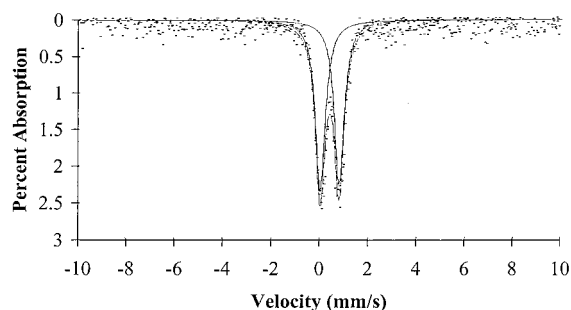

FIGURE 3: Mössbauer spectrum of P_i-reconstituted HoSF. The HoSF core was first reconstituted with 1100 iron atoms using natural abundance Fe^{2+} and made anaerobic, and then excess $^{57}Fe^{2+}$ and P_i were added to reconstitute the P_i layer as described in the text. The sample was then frozen in liquid nitrogen, and Mössbauer spectra were recorded at 77 K. The solid lines are fits for an isomer shift of 0.414 mm/s and a quadrapole splitting of 0.778 mm/s characteristic of $^{57}Fe^{3+}$.

in the initial iron release steps in a manner similar to reductive iron release. Figure 2 provides some insight into this question by showing that phosphate is not removed in a "burst" as with the reductive process. Figure 2 shows that as Fe^{3+} is removed from the HoSF core, there is a small compensatory decrease in phosphate content such that a significant P_i layer always remains associated with the core surface but decreases with core size. The slope of the line (0.16 ± 0.01 P_i:Fe) in Figure 2 provides a quantitative description of this process, suggesting that for every 6.3 iron atoms removed, one phosphate is released.

Core Surface Redox Reactions. Figure 3 is the Mössbauer spectrum of HoSF initially reconstituted with natural abundance iron atoms to which a P_i layer was reconstituted by addition of $^{57}Fe^{2+}$ and P_i as described above. The spectrum shows a quadrapole doublet characteristic of $^{57}Fe^{3+}$. However, when a portion of the sample is reacted with bipyridine, >85% of the added $^{57}Fe^{2+}$ is recovered as $[^{57}Fe(bipy)_3]^{2+}$ as determined by mass spectrometry. It has been observed that α,α-diimine ligands, such as bipy, act as Fe^{3+}-reducing agents when not in strongly acidic media (*16, 17*). As a control, we reacted native HoSF with a large excess of bipy and monitored the color formation of $[Fe(bipy)_3]^{2+}$ over time

and determined that only 0.6 iron atom was released per hour. Since we incubated bipy with our P_i-reconstituted HoSF samples for about 30 min and in light of the mass spectrometric data, it is unlikely that reduction of Fe^{3+} by bipy significantly interferes with this measurement.

Another control reaction (not shown) was conducted with HoSF containing 1000 iron atoms reconstituted from natural abundance iron to which excess $^{57}Fe^{2+}$ was added anaerobically in the absence of phosphate. This control spectrum shows a strong doublet characteristic of $^{57}Fe^{2+}$, and only a small $^{57}Fe^{3+}$ doublet barely above background was observed, suggesting that a small amount of added $^{57}Fe^{2+}$ may be converted to $^{57}Fe^{3+}$ on the P_i-free, iron-reconstituted ferritin mineral core surface. A control reaction mixture containing an identical amount of $^{57}Fe^{2+}$ added to anaerobic buffer was examined under identical conditions to correct for any adventitious $^{57}Fe^{3+}$ that was initially present or produced during the experiment. The amount of $^{57}Fe^{3+}$ that is present in the absence of phosphate is much smaller than that formed in the presence of the P_i-reconstituted cores, indicating that if P_i-free cores do in fact promote surface redox reactions, they do so only weakly.

DISCUSSION

As isolated, all naturally occurring ferritins contain variable amounts of phosphate associated with their mineral cores, suggesting an important but poorly understood role for phosphate in ferritin function. In some cases (HoSF), the phosphate appears to be surface-bound, while in others (AvBFR), it is homogeneously integrated into the mineral core structure (*8*). In both cases, some phosphate is present on the core surface, as evidenced by the enhanced Fe^{2+} binding abilities of both native HoSF and native AvBFR relative to those of their apo forms (*11, 18*). The presence of phosphate is known to (a) affect the crystallinity of the mineral cores (*19*), (b) alter the core redox potentials (*6, 20, 21*), (c) be the site of anaerobic Fe^{2+} binding in holo ferritins (*15, 18, 22*), and (d) promote specific iron redox reactions (*10, 15*). While phosphate strongly influences the reactivity of the mineral cores in various ferritins, the mechanism by which phosphate promotes this reactivity has not been identified. Another poorly understood aspect of ferritin function is the mechanism of phosphate incorporation into ferritin mineral cores in vivo. To understand how ferritins function and how they integrate phosphate into the iron deposition and release reactions they catalyze, it is important to understand how phosphate enters the ferritin interior and is attached to the mineral core surface. The results reported here continue to address the role of phosphate on the surface of HoSF cores by examining how the P_i surface is formed as well as what reactivity this surface layer contributes to ferritin function. The results reported here extend earlier studies of the role of phosphate in ferritin reactivity (*9, 15, 18, 22*).

Reconstitution of the Phosphate Layer in HoSF. The anaerobic addition of both phosphate and Fe^{2+} to iron-reconstituted HoSF cores produces a P_i–Fe^{2+} layer with a P_i:Fe^{2+} stoichiometry of 3.0 ± 1.0 which is independent of the core size (see Tables 1−3). This constant stoichiometry suggests that the same phosphate mineral phase is formed

on the mineral surface throughout the range of core sizes that were studied. As suggested above, increasing core size creates an increasing surface area on which the incoming $Fe^{2+}-P_i$ layer forms. In a recent review of ferrihydrite, Jambor and Dutrizac (*23*) mention that ferrihydrite has a high affinity for phosphate. IR and other studies of phosphate-containing ferrihydrite suggest that phosphate oxygens bind to two singularly coordinated OH groups on the ferrihydrite surface to form a binuclear structure (*24, 25*). Phosphate also inhibits the transformation of ferrihydrite to other iron oxyhydroxides which may be the reason that phosphate "capped" ferrihydrite mineral cores are found in mammalian ferritins (*26, 27*).

Earlier iron deposition measurements (*28*) were reported and analyzed by a simple "free surface" or "crystal growth" model. This model assumes that the core surface is derived from a section of a sphere and appears to be consistent with the behavior shown in Figure 1. This model approximately fits the original kinetic data as well as more recent studies (*13*). The shape of the curve in Figure 1 is consistent with what one would expect when plotting the surface area (reconstituted P_i layer) of a spherical core versus its volume (iron core size). The core surface area increases with increasing core size up to 2500 Fe atoms followed by a decreasing surface area above 2500 Fe atoms as the protein shell begins to interfere with the mineral core, thus decreasing the surface area which results in a decrease in the amounts of P_i and Fe^{2+} that bind. The possibility that an $Fe^{2+}-P_i$ layer is on the mineral core surface is suggested by forming the P_i layer with $^{57}Fe^{2+}$ and then quickly removing it as the $[^{57}Fe(bipy)_3]^{2+}$ complex. Mass spectrometry of the resulting $[Fe(bipy)_3]^{2+}$ shows that more than 85% of the added $^{57}Fe^{2+}$ is released. This "last in—first out" behavior is consistent with a surface reaction.

As the core size approaches the theoretical limit of 4500 iron atoms for loading the HoSF interior, Figure 1 suggests that the amount of bound phosphate does not extrapolate to zero but remains at 50—100 phosphate ions bound to the mineral core. This result implies that some mineral surface is still available to interact with Fe^{2+} and P_i to form a P_i-Fe^{2+} layer even as the volume of the mineral core approaches the limiting volume of the ferritin interior and/or that some phosphate has been trapped in the bulk iron core.

If the P_i layer in HoSF is bound to the surface as is suggested, then the results in Figure 1 and Tables 1 and 2 suggest that the amounts of Fe^{2+} and P_i bound are an indication of the core surface that is available to incoming iron. For example, recent reports (*13*) suggest that at high Fe^{2+} flux, in the absence of phosphate, iron deposition involves catalytic Fe^{2+} oxidation by O_2 on the developing mineral surface. If this view is correct and if Figure 1 and Tables 1 and 2 properly represent core surface variation with core size, then the prediction can be made that the initial rate of Fe^{2+} oxidation by O_2 will increase as the surface area of the growing iron core increases. This prediction is consistent with Figure 6 of Yang et al. (*13*), which shows that as the location of Fe^{2+} oxidation switches from the ferroxidase center to the mineral surface, the rate increases with core size.

We conclude from the results presented in Table 3 that the P_i layer is surface-bound and remains so even after 1000 additional iron atoms have been deposited into the ferritin interior. In both experiments, the added iron appears to be transferred beneath the P_i layer, suggesting that the P_i layer remains surface-bound during core enlargement. These results are consistent with the observed P_i:Fe ratio of 1:10 in HoSF and with the P_i layer carrying out a dynamic, catalytic redox function during iron deposition. Such a process is likely to occur in vivo and suggests that phosphate is performing an important catalytic role in ferritin core formation.

Whatever the actual structure of the iron-reconstituted cores, it is clear that they have variable compositions and/or densities even when reconstituted under similar conditions. This variable core structure is likely the cause of the variable P_i layers represented in Figure 1 and Tables 1 and 2 and in other experiments whose results are not shown. Comparison of our results of the surface-bound P_i with the results of St. Pierre et al. (*29*) who made reconstituted HoSF cores with P_i:Fe ratios of 0.8:1 and 7:1 will be of interest and may give further insights into the in vivo processes involved in forming ferritin cores containing phosphate. It will also be interesting to determine if phosphate is a specific anion for the reconstitution process in ferritins or if other tetrahedral oxyanions (i.e., SO_4^{2-} or SeO_4^{2-}) may also function to reconstitute other oxyanion surfaces (*30*).

Non-Redox Iron Release from Native HoSF. Figure 2 shows the interesting result that as Fe^{3+} is removed aerobically and the core size decreases, the P_i layer adjusts proportionally by expelling phosphate to maintain uniform coverage of the core surface. The mechanism by which the P_i layer assists iron removal remains unknown but appears to be a consequence of the bound P_i layer catalyzing Fe^{3+} transfer from bulk core to protein sites where chelation by DES occurs. There is clearly a contrast between the role of the P_i layer in the reductive iron release reaction where large amounts of the phosphate are lost and its role in the nonreductive iron release process where P_i release remains constant.

Phosphate-Promoted Redox Reactivity. The observation in Figure 3 that anaerobic formation of the P_i layer is accompanied by the reversible oxidation of Fe^{2+} to Fe^{3+} during P_i layer formation suggests an important role for phosphate in promoting redox reactions on the mineral core surface. Once formed anaerobically, the P_i layer and its associated Fe^{3+} can be removed by adding bipy which quantitatively forms $[Fe(bipy)_3]^{2+}$ and releases surface-bound phosphate. However, upon oxidation, the electrons are removed and a fully reconstituted and stable P_i layer remains which behaves as the P_i layer in native HoSF. There are several examples where iron—phosphate compounds have been used as redox catalysts which may provide additional insight into what is happening at the P_i layer—iron core interface (*31–34*).

The results in Table 1 and Figure 3 clearly show that Fe^{2+} interacts with P_i to form an $Fe^{3+}-P_i$ layer with reversible transfer of the electrons presumably to the Fe^{3+} ions in the iron core. The redox potential of the iron in the P_i layer must be lower than the redox potential of the HoSF core iron [-250 mV at pH 7.5 (*20*)] for nearly complete electron transfer to occur from the P_i layer into the core. Upon addition of bipy, the formation of the very stable $[Fe(bipy)_3]^{2+}$ shifts the reversible redox equilibrium from the core back to Fe^{2+} which is then removed during the chelation

Scheme 1
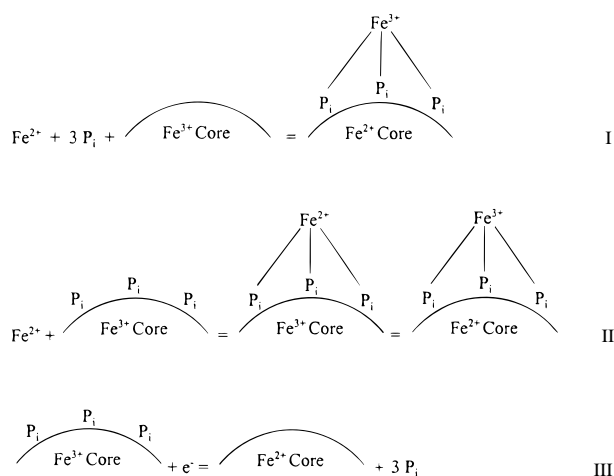
reaction. Similar anaerobic reactions with native ferritins in which added $^{57}Fe^{2+}$ becomes reversibly oxidized on the mineral core surface in a manner similar to that reported here were previously reported (*11*, *15*). The abilities of both native and P_i-reconstituted mineral cores to anaerobically bind Fe^{2+} and display internal and reversible oxidation of the bound Fe^{2+} are further indications that the reconstituted P_i layer behaves like that produced in vivo.

Reconstituting the P_i layer is a complex process that involves Fe^{2+}, P_i, and core interactions which result in Fe^{2+} being reversibly oxidized with the electron being transferred to the iron atoms in the mineral core. The reactions required to reconstitute the P_i layer in HoSF are shown schematically by reaction I in Scheme 1 and have parallels (yet distinct differences) with other reported reactions of the native P_i layer in HoSF. For example, reaction II represents the anaerobic binding of Fe^{2+} to a preexisting, native HoSF P_i layer (*10*) and illustrates the reversible oxidation of bound Fe^{2+} to Fe^{3+}. The multistep binding/redox reaction II can be reversed by reaction with bipy, with retention of the original P_i layer and formation of $[Fe(bipy)_3]^{2+}$ in a reaction that overall is similar to reaction I (*10*). Reaction III represents yet another P_i layer reaction showing that a reduction of 10% of the core iron atoms by DT mobilizes 60% of the bound phosphate present in native HoSF (*12*). This reaction suggests that reduction may occur at iron atoms specifically associated with bound phosphate. Thus, it is becoming clear that rather unusual and complex iron binding and redox activity occur at the P_i−Fe core interface which is likely to be associated with ferritin function. Because similar binding and redox reactivity are observed in bacterial ferritins containing homogeneously distributed phosphate in the core, a more detailed comparison of surface-bound phosphate and uniformly distributed phosphate in various ferritin types will be of interest in further elucidating the role of phosphate.

Fe^{2+} binds to native holo ferritin in direct proportion to the amount of phosphate associated with the native core (*22*). In contrast, column 2 of Table 2 shows that Fe^{2+} binds only to a limited degree to iron-reconstituted HoSF in the absence of phosphate, with a value of 7.2 ± 1.0 Fe^{2+} atoms/HoSF which is independent of core size. This result is consistent with a previous report that 8.0 ± 0.5 Fe^{2+} atoms bind anaerobically per apo HoSF (*10*). Formation of a P_i layer

on the cores of reconstituted HoSF by the method reported here creates levels of phosphate comparable to those found in native HoSF containing comparable core sizes. For example, native 1 and native 2 in Table 3 have 2010 and 1800 iron atoms and 445 and 392 phosphate groups present, respectively, while the reconstituted sample in Table 1 had $\sim$612 and $\sim$ 483 phosphate groups, respectively, for comparable core sizes. Column 3 of Tables 1 and 2 shows that the extent of Fe^{2+} binding increases in direct proportion to the amount of reconstituted phosphate present, and the last column of each table shows similar Fe^{2+}:P_i binding stoichiometry. These results are consistent in showing that the behavior of Fe^{2+} binding to P_i-reconstituted HoSF is nearly identical to that observed with native HoSF. Column 3 of Tables 1 and 2 shows that a stoichiometry of 3.0 phosphates are required to bind each Fe^{2+} in P_i-reconstituted HoSF, a result nearly identical to that reported for Fe^{2+} binding to native HoSF (*12*, *15*) and also consistent with the EPR studies of Cheng and Chasteen (*9*). The results in Table 2 provide strong evidence that P_i-reconstituted HoSF cores are equivalent to native HoSF cores.

The in vitro conditions used here to reconstitute the P_i layer are quite specific, and if the same process occurs in vivo, then a number of questions arise regarding P_i layer formation in vivo. Is the phosphate added only after the iron core has been formed? If so, then the ferritin must simultaneously have available to it an anaerobic environment, Fe^{2+}, and a supply of phosphate. Is the P_i layer added early in core formation which then "floats" on the surface during subsequent iron deposition as the data in Table 3 demonstrate? If this is the case, then as the core enlarges phosphate must be added to the growing core as shown in Figure 1. These are stringent requirements and may or may not be consistent with cellular physiology, so we continue to investigate other P_i reconstitution methods. However, the method described here seems to be a viable method for reconstituting the P_i layer with characteristics similar if not identical to those of native ferritins and should be of value in future experiments.

REFERENCES

1. Waldo, G. S., and Theil, E. C. (1996) *Compr. Supramol. Chem. 5*, 65−89.
2. Proulx-Curry, P. M., and Chasteen, N. D. (1995) *Coord. Chem. Rev. 144*, 347−368.
3. Harrison, P. M., and Arosio, P. (1996) *Biochim. Biophys. Acta 1275*, 161−203.
4. Treffry, A., Harrison, P. M., Cleton, M. I., De Bruijn, W. C., and Mann, S. (1987) *J. Inorg. Biochem. 31*, 1−6.
5. Wade, V. J., Treffry, A., Laulhere, J. P., Bauminger, E. R., Cleton, M. I., Mann, S., Briat, J. F., and Harrison, P. M. (1993) *Biochim. Biophys. Acta 1161*, 91−96.
6. Watt, G. D., Frankel, R. B., Papaefthymiou, G. C., Spartalian, K., and Stiefel, E. I. (1986) *Biochemistry 25*, 4330−4336.
7. Treffry, A., and Harrison, P. M. (1978) *Biochem. J. 171*, 313−320.
8. Rohrer, J. S., Islam, Q. T., Watt, G. D., Sayers, D. E., and Theil, E. C. (1990) *Biochemistry 29*, 259−264.
9. Cheng, Y. G., and Chasteen, N. D. (1991) *Biochemistry 30*, 2947−2953.
10. Jacobs, D., Watt, G. D., Frankel, R. B., and Papaefthymiou, G. C. (1989) *Biochemistry 28*, 9216−9221.
11. Watt, G. D., Frankel, R. B., Jacobs, D., Heqing, H., and Papaefthymiou, G. C. (1992) *Biochemistry 31*, 5672−5679.

12. Huang, H., Watt, R. K., Frankel, R. B., and Watt, G. D. (1993) *Biochemistry 32*, 1681−1687.

13. Yang, X., Chen-Barrett, Y., Arosio, P., and Chasteen, N. D. (1998) *Biochemistry 37*, 9743−9750.

14. Treffry, A., Banyard, S. H., Hoare, R. J., Harrison, P. M., Brown, E. B., Aisen, P., and Fielding, J. (1977) *Proteins Iron Metab., [Proc. Int. Meet.], 3rd*, 3−11.

15. Jacobs, D. L., Watt, G. D., Frankel, R. B., and Papaefthymiou, G. C. (1989) *Biochemistry 28*, 1650−1655.

16. Pehkonen, S. (1995) *Analyst 120*, 2655.

17. Monsted, O., and Nord, G. (1991) *Adv. Inorg. Chem. 37*, 381.

18. Watt, R. K., Frankel, R. B., and Watt, G. D. (1992) *Biochemistry 31*, 9673−9679.

19. Mann, S., Bannister, J. V., and Williams, R. J. P. (1986) *J. Mol. Biol. 188*, 225−232.

20. Watt, G. D., Frankel, R. B., and Papaefthymiou, G. C. (1985) *Proc. Natl. Acad. Sci. U.S.A. 82*, 3640−3643.

21. Watt, G. D., Jacobs, D., and Frankel, R. B. (1988) *Proc. Natl. Acad. Sci. U.S.A. 85*, 7457−7461.

22. Huang, H., Watt, R. K., Watt, G. D., and Frankel, R. B. (1993) *Xiamen Daxue Xuebao, Ziran Kexueban 32*, 628−633.

23. Jambor, J. L., and Dutrizac, J. E. (1998) *Chem. Rev. 98*, 2549−2585.

24. Willett, I. R., Chartres, C. J., and Nguyen, T. T. (1988) *J. Soil Sci. 39*, 275.

25. Manceau, A., and Charlet, L. J. (1994) *J. Colloid Interface Sci. 168*, 87.

26. Cornell, R. M., Giovanoli, R., and Schindler, P. W. (1987) *Clays Clay Miner. 35*, 21.

27. Barron, V., Galvez, N., Hochella, M. F., Jr., and Torrent, J. (1997) *Am. Mineral. 82*, 1091.

28. Treffry, A., Sowerby, J. M., and Harrison, P. M. (1978) *FEBS Lett. 95*, 221−224.

29. St. Pierre, T. G., Chan, P., Bauchspiess, K. R., Webb, J., Betteridge, S., Walton, S., and Dickson, D. P. E. (1996) *Coord. Chem. Rev. 151*, 125−143.

30. Parfitt, R. L., and Smart, R. S. C. (1978) *Soil Sci. Soc. Am. J. 42*, 48.

31. Gadgil, M. M., and Kulshreshtha, S. K. (1994) *J. Solid State Chem. 111*, 357−364.

32. Muneyama, E., Kunishige, A., Ohdan, K., and Ai, M. (1994) *J. Mol. Catal. 89*, 371−381.

33. Ai, M., Muneyama, E., Kunishige, A., and Ohdan, K. (1994) *Bull. Chem. Soc. Jpn. 67*, 551−556.

34. Ai, M., Muneyama, E., Kunishige, A., and Ohdan, K. (1994) *Catal. Lett. 24*, 355−362.